Journal of Southeast University (English Edition) Vol. 25, No. 4, pp. 501 – 505 Dec. 2009 ISSN 1003—7985

Improved finite difference method for pressure distribution of aerostatic bearing

Zheng Shufei Jiang Shuyun

(School of Mechanical Engineering, Southeast University, Nanjing 211189, China)

Abstract: An improved finite difference method (FDM) is described to solve existing problems such as low efficiency and poor convergence performance in the traditional method adopted to derive the pressure distribution of aerostatic bearings. A detailed theoretical analysis of the pressure distribution of the orifice-compensated aerostatic journal bearing is presented. The nonlinear dimensionless Reynolds equation of the aerostatic journal bearing is solved by the finite difference method. Based on the principle of flow equilibrium, a new iterative algorithm named the variable step size successive approximation method is presented to adjust the pressure at the orifice in the iterative process and enhance the efficiency and convergence performance of the algorithm. A general program is developed to analyze the pressure distribution of the aerostatic journal bearing by Matlab tool. The results show that the improved finite difference method is highly effective, reliable, stable, and convergent. Even when very thin gas film thicknesses (less than 2 μm) are considered, the improved calculation method still yields a result and converges fast.

Key words: aerostatic bearing; pressure distribution; Reynolds equation; finite difference method; variable step size

Compared with the traditional rolling bearings and oil bearings, gas bearings have the advantages of lower heat generation, lower wear and friction, lower noise, less contamination and higher precision. Due to their advantages over rolling bearings and oil bearings, gas bearings are widely used in precision machine tools, semiconductor wafer processing machines, high-speed motors, etc.

Considerable efforts have been devoted to the research of the pressure distribution of gas bearings. The engineering algorithm[1-2], which assumes that the flow in the gas film is one dimensional, was developed in earlier studies. This algorithm is simple, but its error is large when thin gas film thicknesses are considered. With the development of computers, the finite element method (FEM)[2-4] and the finite difference method (FDM)[5-8] have become two major methods to solve the Reynolds equation. The FEM is suitable for the complex geometry of bearings and it has been successfully used. However, it is an extremely complicated work to calculate the pressure distribution of the aerostatic journal bearing by using the FEM, and it is also difficult to develop a general program by this method.

Received 2009-06-25.

Biographies: Zheng Shufei (1985—), male, graduate; Jiang Shuyun (corresponding author), male, doctor, professor, jiangshy@seu.edu.cn.

Foundation items: The National Natural Science Foundation of China (No. 50475073, 50775036), the High Technology Research Program of Jiangsu Province (No. BG2006035).

Citation: Zheng Shufei, Jiang Shuyun. Improved finite difference method for pressure distribution of aerostatic bearing[J]. Journal of Southeast University (English Edition), 2009, 25(4): 501 – 505.

The FDM has many advantages. The computational grid is simple and the computational process is more convenient than the FEM. By using this method, it is also easier to write general programs. However, low efficiency and poor convergence performance are the main disadvantages of the FDM. Zhang[7] used the FDM to analyze the pressure distribution of aerostatic journal bearings. But the convergence performance of his algorithm is poor and it is not suitable for thin gas film thicknesses. Lo et al.[8] also studied the FDM, and the iterative rate cutting method[2] was adopted. The iterative rate cutting method converges to a solution even when very thin film thicknesses are considered. However, the computational efficiency of the algorithm is low. Furthermore, the iterative rate cutting method is complicated. For this reason, the objective of this paper is to examine the problem.

1 Mathematical Modeling

1.1 Reynolds equation and its non-dimensional form

The geometry of the aerostatic journal bearing is shown in Fig. 1. The dimension of the gas film thickness is much less than that of the diameter of the bearing. Hence, the surface curvature of the cylinder can be neglected and the gas film is expanded along the axis of $\alpha = 0$ as shown in Fig. 2.

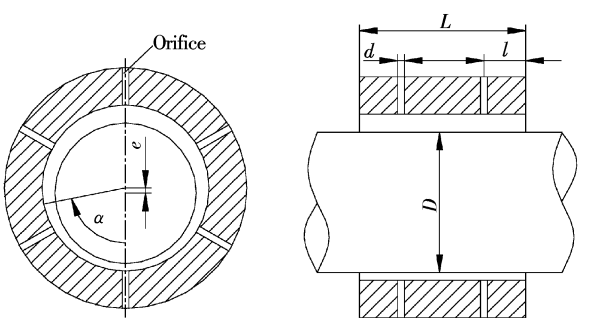

Fig. 1 Geometry of the aerostatic journal bearing coincidence boundary

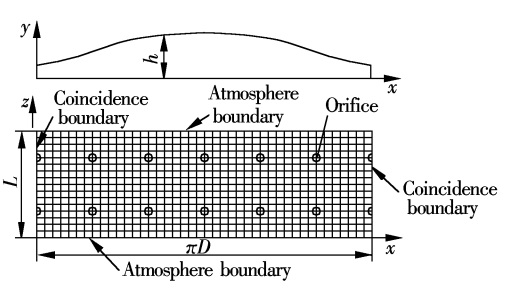

Fig. 2 Expanded gas film and the computational grid of the aerostatic journal bearing

The main purpose of this paper is to propose an efficient iterative algorithm. For simplicity, the aerostatic bearing without considering the dynamic pressure effect is chosen to show this computational process. It is assumed that the flow in the gas film is isothermal. The pressure distribution in the gas film is modeled by the compressible Reynolds equation as[2]

$$\frac{\partial}{\partial x}\left(h^3\frac{\partial p^2}{\partial x}\right)+\frac{\partial}{\partial z}\left(h^3\frac{\partial p^2}{\partial z}\right)=0 \tag{1}$$

The dimensionless form of the Reynolds equation is given as

$$\frac{\partial}{\partial \bar{x}}\left(\bar{h}^3\frac{\partial \bar{p}^2}{\partial \bar{x}}\right)+\frac{\partial}{\partial \bar{z}}\left(\bar{h}^3\frac{\partial \bar{p}^2}{\partial \bar{z}}\right)=0 \tag{2}$$

where $\bar{p}=p/p_a$, $\bar{h}=h/h_0=1-\varepsilon\cos(x/R)$, $\bar{x}=x/l$, $\bar{z}=z/l$, $R=D/2$, $\varepsilon=e/h_0$. Eq. (2) can be written as

$$\frac{\partial}{\partial \bar{x}}\left(\bar{h}^3\frac{\partial \bar{f}}{\partial \bar{x}}\right)+\frac{\partial}{\partial \bar{z}}\left(\bar{h}^3\frac{\partial \bar{f}}{\partial \bar{z}}\right)=0 \tag{3}$$

where $\bar{p}^2=\bar{f}$.

1.2 Discretization of the Reynolds equation

Eq. (3) can be written in an expanded form,

$$\left(\frac{\partial \bar{h}^3}{\partial \bar{x}}\frac{\partial \bar{f}}{\partial \bar{x}}+\bar{h}^3\frac{\partial^2 \bar{f}}{\partial \bar{x}^2}\right)+\left(\frac{\partial \bar{h}^3}{\partial \bar{z}}\frac{\partial \bar{f}}{\partial \bar{z}}+\bar{h}^3\frac{\partial^2 \bar{f}}{\partial \bar{z}^2}\right)=0 \tag{4}$$

By using the five point finite difference scheme, we obtain

$$a_{i,j}\frac{\bar{f}_{i+1,j}-\bar{f}_{i-1,j}}{2\Delta\bar{x}}+\bar{h}^3_{i,j}\frac{\bar{f}_{i+1,j}-2\bar{f}_{i,j}+\bar{f}_{i-1,j}}{(\Delta\bar{x})^2}+\bar{h}^3_{i,j}\frac{\bar{f}_{i,j+1}-2\bar{f}_{i,j}+\bar{f}_{i,j-1}}{(\Delta\bar{z})^2}=0 \tag{5}$$

where $a_{i,j}=\left[\frac{3\bar{h}^2\varepsilon l}{R}\sin\left(\frac{x}{R}\right)\right]_{i,j}$.

Eq. (5) can be written as

$$A_{i,j}\bar{f}_{i+1,j}+B_{i,j}\bar{f}_{i-1,j}+C_{i,j}\bar{f}_{i,j}+D_{i,j}\bar{f}_{i,j-1}+E_{i,j}\bar{f}_{i,j+1}=0 \tag{6}$$

where $A_{i,j}=\frac{\bar{h}^3_{i,j}}{(\Delta\bar{x})^2}+\frac{a_{i,j}}{2\Delta\bar{x}}$, $B_{i,j}=\frac{\bar{h}^3_{i,j}}{(\Delta\bar{x})^2}-\frac{a_{i,j}}{2\Delta\bar{x}}$, $C_{i,j}=\frac{-2\bar{h}^3_{i,j}}{(\Delta\bar{x})^2}+\frac{-2\bar{h}^3_{i,j}}{(\Delta\bar{z})^2}$, $D_{i,j}=\frac{\bar{h}^3_{i,j}}{(\Delta\bar{z})^2}$, $E_{i,j}=\frac{\bar{h}^3_{i,j}}{(\Delta\bar{z})^2}$.

1.3 Boundary conditions

The boundary conditions are illustrated in Fig. 2; i. e., the atmosphere boundary condition is $\bar{f}\,|_{z=0}=(p_{i,j}/p_a)^2=1$, $\bar{f}\,|_{z=L}=(p_{i,j}/p_a)^2=1$; the coincidence boundary is $\bar{f}\,|_{x=0}=\bar{f}\,|_{x=\pi D}$.

2 Principle of Flow Equilibrium

2.1 Mass inflow rate

Adopting the assumptions of an adiabatic process and a non-viscous flow, the mass inflow rate through an orifice is given as[2]

$$m_{in}=Ap_0\phi\sqrt{\frac{2\rho_0}{p_0}}\psi$$

$$\psi=\begin{cases}\left[\frac{k}{2}\left(\frac{2}{k+1}\right)^{(k+1)/(k-1)}\right]^{1/2} & \beta=\frac{p}{p_0}\leqslant\beta_k\\ \left\{\frac{k}{k-1}\left[\left(\frac{p}{p_0}\right)^{2/k}-\left(\frac{p}{p_0}\right)^{(k+1)/k}\right]\right\}^{1/2} & \beta=\frac{p}{p_0}>\beta_k\end{cases} \tag{7}$$

where A is the cross-sectional area of the orifice, k is the ratio of specific heat, p_0 is the supplied pressure, ϕ is the coefficient of the mass flow rate through the orifice, and $\beta_k=(2/(k+1))^{k/(k-1)}$.

2.2 Mass outflow rate

As shown in Fig. 3, the mass flow rate through Δz in the x direction is as

$$m_x=\int_0^h\rho u\Delta z\mathrm{d}y=\int_0^h\rho\left(-\frac{1}{2\eta}\frac{\partial p}{\partial x}\right)y(h-y)\Delta z\mathrm{d}y=\rho\frac{-1}{2\eta}\frac{\partial p}{\partial x}\Delta z\frac{h^3}{6} \tag{8}$$

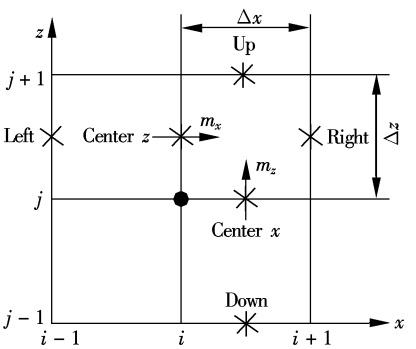

Fig. 3 Calculation of mass outflow rate

The flow in the gas film is isothermal. Hence we obtain

$$\frac{p}{\rho}=\frac{p_a}{\rho_a} \tag{9}$$

Substituting Eq. (9) into Eq. (8), we can obtain

$$m_x=p\frac{\rho_a}{p_a}\frac{-1}{2\eta}\frac{\partial p}{\partial x}\Delta z\frac{h^3}{6} \tag{10}$$

The pressure and pressure gradient can be approximated as

$$\left.\begin{aligned}p_{centerz}&=\frac{p_{i,j}+p_{i,j+1}}{2}\\ \frac{\partial p}{\partial x}&=\frac{p_{right}-p_{left}}{2\Delta x}\\ p_{left}&=\frac{p_{i-1,j}+p_{i-1,j+1}}{2}\\ p_{right}&=\frac{p_{i+1,j}+p_{i+1,j+1}}{2}\end{aligned}\right\} \tag{11}$$

Substituting Eq. (11) into Eq. (10), we can obtain

$$m_x=\frac{\Delta z}{\Delta x}\frac{-h^3}{24\eta}\frac{\rho_a}{p_a}p_{centerz}(p_{right}-p_{left}) \tag{12}$$

Similarly, the mass flow rate through Δx in the z direction is as

$$m_z = \frac{\Delta x}{\Delta z}\frac{-h^3}{24\eta}\frac{\rho_a}{p_a}p_{centerx}(p_{up} - p_{down}) \tag{13}$$

2.3 Flow rate difference

The flow equilibrium region of an orifice is shown in Fig. 4. The flow rate difference of the region is

$$\Delta m = m_{in} - m_{out} = m_{in} - (m_1 + m_2 + m_3 + m_4) \tag{14}$$

where m_1, m_2, m_3 and m_4 can be determined with the help of Eqs. (12) and (13).

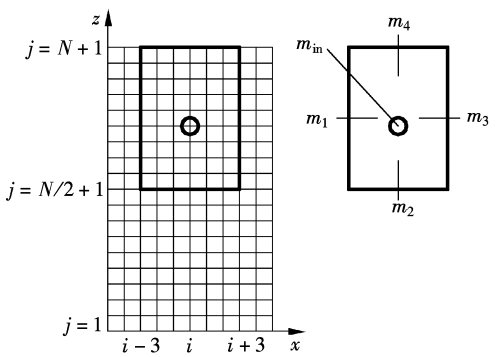

Fig. 4 Flow equilibrium region of an orifice

The relative error of the flow equilibrium region is defined as

$$E = \frac{\Delta m}{m_{in}} \tag{15}$$

2.4 Variable step size successive approximation method

Before solving the Reynolds equation, the pressure at each orifice should be assumed, which is called the iterative initial value. Then, the Reynolds equation is solved and the pressure distribution of the aerostatic journal bearing can be obtained. The relative error of the flow equilibrium region at each orifice is obtained from Eq. (15). If any of the relative errors cannot meet the calculation precision (e. g., 10^{-6}), the pressure at each orifice should be adjusted and the Reynolds equation is solved once again. This cycle continues until the relative error of the flow equilibrium region at each orifice is less than the calculation precision.

In order to enhance the computational efficiency and the convergence of the FDM, a variable step size successive approximation method is presented to adjust the pressure at the orifice during the iteration. The calculation process of the variable step size successive approximation method to adjust the pressure at an orifice is shown in Fig. 5. In Fig. 5, m_{in} and m_{out} are the mass inflow rate curve and the mass outflow rate curve of the flow equilibrium region, respectively, and the intersection point of the two curves (β_0) is the true value of the dimensionless pressure at the orifice.

As shown in Fig. 5, β_1 is the iterative initial value of the pressure at an orifice. After the first calculation of the Reynolds equation, the relative error of the flow equilibrium region at the orifice is obtained by using Eq. (15). Because the sign of the relative error is positive, β_1 is increased by a step size K. Then, the second calculation of the Reynolds equation is carried out, and the same process as the first calculation is performed. When the pressure at the orifice reaches β_4, the sign of the relative error changes from positive to negative, and then the step size K is decreased to $K/10$. Because the sign of the relative error is negative now, β_4 is decreased by the new step size $K/10$. Then the calculation continues. During the iteration, when the sign of the relative error changes, the new step size decreases to 1/10 that of the last step. This computational process continues until the relative error of the flow equilibrium region at each orifice is less than the calculation precision.

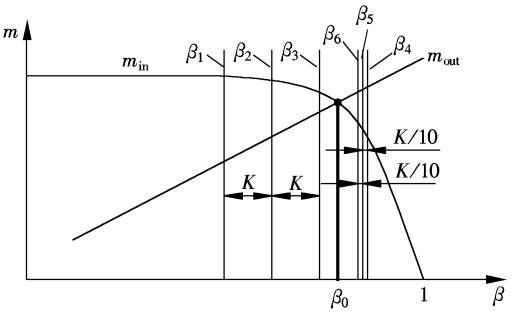

Fig. 5 Schematic diagram of the variable step size successive approximation method

3 Results and Discussions

Based on the above theory, a computer program has been developed by using Matlab to analyze the pressure distribution of the aerostatic journal bearing. The computational flow diagram is shown in Fig. 6.

The parameters of bearings are chosen as follows: $D = L = 250$ mm, number of orifices $n = 24$, $p_0 = 4 \times 10^5$ Pa, $d = 0.3$ mm, radius clearance $h_0 = 30$ μm, calculation precision $E_0 = 10^{-6}$. With the eccentricity ratios changed from 0.1 to 0.9, the load capacity of the aerostatic journal bearing is simulated by using the improved FDM. The simulated results are also compared with that of the engineering algorithm, which derives from Ref. [2].

It can be seen from Tab. 1 that with the increase of eccentricity ratios, the relative differences of the two methods tends to increase. This is because the flow in the gas film is assumed to be one dimensional in the engineering algorithm, which produces big errors for large eccentricity ratios.

Tab. 1 Comparison between the improved FDM and the engineering algorithm

Eccentricity ratio	Load capacity/kN		Relative difference/%
	Engineering algorithm	Improved FDM	
0.1	1.498	1.465	2.20
0.2	2.936	2.834	3.47
0.3	4.241	4.031	4.95
0.4	5.325	5.013	5.86
0.5	6.156	5.784	6.04
0.6	6.762	6.371	5.78
0.7	7.204	6.799	5.62
0.8	7.541	7.081	6.10
0.9	7.807	7.206	7.70

Fig. 7 illustrates the pressure distribution of the aerostatic journal bearing for the eccentricity ratio of $\varepsilon = 0.3$. It can be seen that the pressure at the orifice is at local maximum.

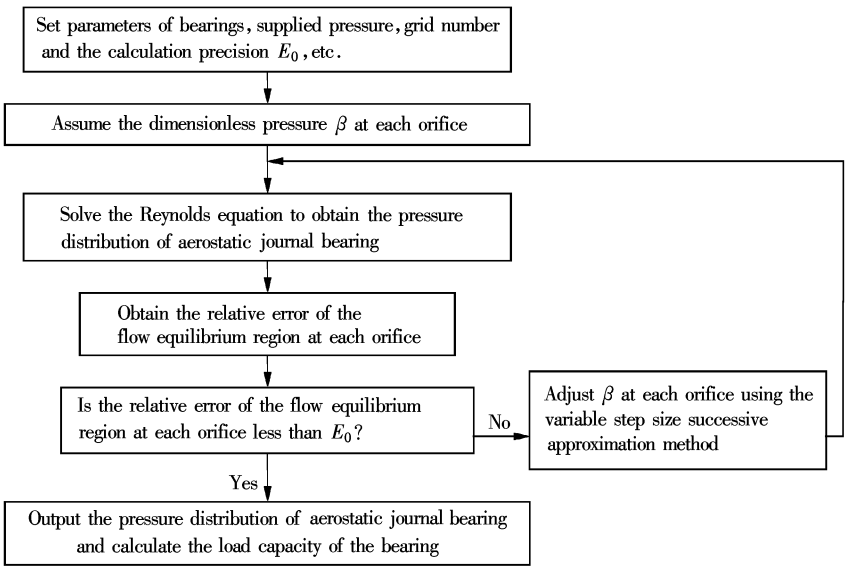

Fig. 6 The computational flow diagram

The pressure at the orifice, where the gas film thicknesses are thinner, is higher. It is because the thinner the gas film, the larger the air resistance. This can result in a lower pressure drop through the orifice; hence the pressure at the orifice is higher.

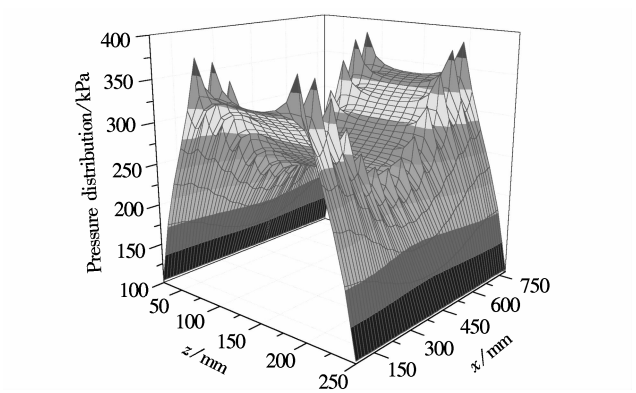

Fig. 7 The pressure distribution of the aerostatic journal bearing ($\varepsilon = 0.3$)

Under the condition of $\varepsilon = 0.1$ and $E_0 = 10^{-6}$, for different radial radius clearances, the Reynolds equation is solved and the times of iteration are listed in Tab. 2. The convergence of the improved FDM is also compared with that of the traditional FDM presented in Ref. [8].

Tab. 2 Convergence comparison between improved FDM and traditional FDM

Radial radius clearance/μm	Times of iteration	
	Improved FDM	Traditional FDM
20	89	698
16	78	1 262
12	87	1 658
8	127	1 785
6	85	1 803
2	107	Not simulated
1	124	Not simulated

It can be seen from Tab. 2 that compared with the traditional FDM, the variable step size successive approximation method presented in this paper can significantly improve the computational efficiency and the convergence of the FDM. Especially, for the 1 μm thick gas film, the advanced calculation method still yields a result and converges fast.

4 Conclusion

In this paper, an improved FDM for the pressure distribution of the orifice-compensated aerostatic journal bearing is presented. Based on the principle of flow equilibrium, a new variable step size successive approximation iterative algorithm is presented to adjust the pressure at the orifice in the iterative process. Compared with the traditional FDM, the variable step size successive approximation iterative algorithm has properties of high computational efficiency and rapid convergence. For very thin gas film thicknesses, the presented calculation method can still yield a result and converge fast. A general program is developed to analyze the pressure distribution of the aerostatic journal bearing by using the Matlab tool, which can be used for gas bearing design and application.

References

[1] Khatait J P, Lin W, Lin W J. Design and development of orifice-type aerostatic thrust bearing [J]. *SIMTech Technical Reports*, 2005, **6**(1): 7 - 12.

[2] Liu D, Liu Y H, Chen S J. *Aerostatic gas lubrication*[M]. Harbin: Harbin Institute of Technology Press, 1990. (in Chinese)

[3] Li S S, Liu D. Analysis of the dynamics of precision centrifuge spindle system with the externally pressurized gas bearing [J]. *Chinese Journal of Mechanical Engineering*, 2005, **41**(2): 28 - 32. (in Chinese)

[4] Awasthi R K, Jain S C, Sharma S C. Finite element analysis of orifice-compensated multiple hole-entry worn hybrid journal bearing [J]. *Finite Elements in Analysis and Design*, 2006, **42**(14): 1291 - 1303.

[5] Wang X, Yamaguchi A. Characteristics of hydrostatic bearing/seal parts for water hydraulic pumps and motors. Part 1: experiment and theory [J]. *Tribology International*, 2002, **35**(7): 425 - 433.

[6] Abdel-Rahman G M. Studying fluid squeeze characteristics for aerostatic journal bearing [J]. *Physica B*, 2008, **403**(13/14/15/16): 2390 - 2393.

[7] Zhang J W. Numerical analysis and application research of gas-lubricated bearings [D]. Xi'an: School of Mechanical Engineering of Xi'an Institute of Technology, 2002. (in Chinese)

[8] Lo C Y, Wang C C, Lee Y H. Performance analysis of high-speed spindle aerostatic bearings [J]. *Tribology International*, 2005, **38**(1): 5 - 14.

一类改进的气体静压轴承压力场分布有限差分算法

郑书飞　　蒋书运

(东南大学机械工程学院, 南京 211189)

摘要: 针对传统的静压气体轴承压力分布算法效率较低或收敛性较差等问题, 提出了一类改进的有限差分计算方法. 以小孔节流式的径向静压气体轴承的压力分布为对象, 采用有限差分法求解非线性雷诺气体润滑方程; 根据流量平衡原理, 提出了一种新型变步长逐步逼近迭代算法, 用于修正迭代过程中的供气口出口压力, 提高算法的效率和收敛性; 基于 Matlab 工具, 开发了一套通用的径向静压气体轴承的压力场分布计算软件. 算例结果表明: 所提出的改进有限差分法计算效率高, 稳定性好, 收敛快; 对于小间隙(小于 2 μm)气膜, 此方法仍然有效并快速收敛.

关键词: 气体静压轴承; 压力场分布; 雷诺方程; 有限差分法; 变步长

中图分类号: TH133.35